

# Synthesis of Calcium Orthophosphates by Chemical Precipitation in Aqueous Solutions: The Effect of the Acidity, Ca/P Molar Ratio, and Temperature on the Phase Composition and Solubility of Precipitates

## **Authors:**

Mykola V. Nikolenko, Kateryna V. Vasylenko, Victoria D. Myrhorodska, Andrii Kostyniuk, Blaž Likozar

*Date Submitted:* 2020-12-28

*Keywords:* solubility isotherm, solubility product, Ca-deficient hydroxyapatite, hydroxyapatite, wet chemical precipitation

## *Abstract:*

Studies on chemical precipitation of the calcium orthophosphates have shown that their phase compositions do not vary depending on molar ratio Ca/P but are sensitive to solutions acidity and temperature. These are two key factors that determine the phase transformation progress of metastable phases into less soluble precipitates of the phosphates. It was proposed to compare calcium orthophosphates solubility products with calcium cations quantities in their formulas. It was found that there was a linear correlation between calcium orthophosphates specific solubility products and their molar ratios Ca/P if hydroxyapatite and its Ca-deficient forms were excluded from consideration. It was concluded that the relatively large deviations of their solubility products from the found correlation should be thought of as erroneous data. That is why solubility products were changed in accordance with correlation dependence: pKS for hydroxyapatite was 155, pKS for Ca-deficient hydroxyapatites was 114?155. The solubility isotherms, which were calculated on the basis of the corrected pKS values, coincided with the experimental data on solid-phase titration by Pan and Darvell.

*Record Type:* Published Article

*Submitted To:* LAPSE (Living Archive for Process Systems Engineering)

*Citation (overall record, always the latest version):*

LAPSE:2020.1284

*Citation (this specific file, latest version):*

LAPSE:2020.1284-1

*Citation (this specific file, this version):*




LAPSE:2020.1284-1v1

*DOI of Published Version:* <https://doi.org/10.3390/pr8091009>

*License:* Creative Commons Attribution 4.0 International (CC BY 4.0)

Article

# Synthesis of Calcium Orthophosphates by Chemical Precipitation in Aqueous Solutions: The Effect of the Acidity, Ca/P Molar Ratio, and Temperature on the Phase Composition and Solubility of Precipitates

Mykola V. Nikolenko <sup>1</sup>, Kateryna V. Vasylenko <sup>1</sup>, Victoria D. Myrhorodska <sup>1</sup>,  
Andrii Kostyniuk <sup>2,\*</sup> and Blaž Likozar <sup>2,3</sup>

<sup>1</sup> Faculty of Chemical Technologies and Ecology, Ukrainian State University of Chemical Technology, Gagarin Avenue 8, 49005 Dnipro, Ukraine; n\_nikolenko@ukr.net (M.V.N.); katrin30.01.92@gmail.com (K.V.V.); mirgorodskaya.viktoria@gmail.com (V.D.M.)

<sup>2</sup> Department of Catalysis and Chemical Reaction Engineering, National Institute of Chemistry, Hajdrihova 19, 1001 Ljubljana, Slovenia; blaz.likozar@ki.si

<sup>3</sup> Faculty of Chemistry and Chemical Technology, University of Ljubljana, Večna pot 113, 1001 Ljubljana, Slovenia

\* Correspondence: andrii.kostyniuk@ki.si; Tel.: +386-01-476-05-40

Received: 10 July 2020; Accepted: 13 August 2020; Published: 19 August 2020



**Abstract:** Studies on chemical precipitation of the calcium orthophosphates have shown that their phase compositions do not vary depending on molar ratio Ca/P but are sensitive to solutions acidity and temperature. These are two key factors that determine the phase transformation progress of metastable phases into less soluble precipitates of the phosphates. It was proposed to compare calcium orthophosphates solubility products with calcium cations quantities in their formulas. It was found that there was a linear correlation between calcium orthophosphates specific solubility products and their molar ratios Ca/P if hydroxyapatite and its Ca-deficient forms were excluded from consideration. It was concluded that the relatively large deviations of their solubility products from the found correlation should be thought of as erroneous data. That is why solubility products were changed in accordance with correlation dependence:  $pK_S$  for hydroxyapatite was 155,  $pK_S$  for Ca-deficient hydroxyapatites was 114–155. The solubility isotherms, which were calculated on the basis of the corrected  $pK_S$  values, coincided with the experimental data on solid-phase titration by Pan and Darvell.

**Keywords:** wet chemical precipitation; hydroxyapatite; Ca-deficient hydroxyapatite; solubility product; solubility isotherm

## 1. Introduction

Calcium orthophosphates are of particular interest among the other phosphorus inorganic compounds because calcium orthophosphates are the mineral basis of the bone tissues and that is why they are thought of as promising biomaterials with perfect biocompatibility. They are used in regenerative medicine, orthopedics, conservative dentistry, dental surgery, for example, as coatings of dental implants, dental cement, bone filler materials for the cavity's reconstruction in maxillofacial surgery [1–8]. Questions of the calcium orthophosphates synthesis and dissolution are under an intensive study by researchers in various fields of science and according to data from Dorozhkin [1], as of today, the total number of publications concerning calcium orthophosphates has increased to 45 thousand with an annual increase of approximately 2 thousand.

It has been reliably proving [9–11] that the five specific calcium orthophosphates with a molar ratio Ca/P in the range of 0.5 to 1.67 are possible to be obtained in the  $\text{Ca}(\text{OH})_2\text{-H}_3\text{PO}_4\text{-H}_2\text{O}$  system, namely, monocalcium phosphate monohydrate  $\text{Ca}(\text{H}_2\text{PO}_4)_2\cdot\text{H}_2\text{O}$ , dicalcium phosphate dihydrate  $\text{CaHPO}_4\cdot 2\text{H}_2\text{O}$ , dicalcium phosphate anhydrous  $\text{CaHPO}_4$ , octacalcium phosphate  $\text{Ca}_8(\text{HPO}_4)_2(\text{PO}_4)_4\cdot 5\text{H}_2\text{O}$ , and hydroxyapatite  $\text{Ca}_{10}(\text{PO}_4)_6(\text{OH})_2$ . Three more similar compounds can also be logically attributed to this system, namely, monocalcium phosphate anhydrous  $\text{Ca}(\text{H}_2\text{PO}_4)_2$ ,  $\alpha$ -tricalcium phosphate  $\alpha\text{-Ca}_3(\text{PO}_4)_2$ , and  $\beta$ -tricalcium phosphate  $\beta\text{-Ca}_3(\text{PO}_4)_2$ , but they are not precipitated from the aqueous solutions. Additionally, compounds of variable compositions are also considered as individual compounds: amorphous calcium phosphate  $\text{Ca}_x\text{H}_y(\text{PO}_4)_z\cdot n\text{H}_2\text{O}$  (with molar ratio  $\text{Ca}/\text{P} = 1.2\text{--}2.2$ ) and calcium-deficient hydroxyapatite  $\text{Ca}_{10-x}(\text{HPO}_4)_x(\text{PO}_4)_{6-x}(\text{OH})_{2-x}$  (with molar ratio  $\text{Ca}/\text{P} = 1.50\text{--}1.67$ ) [1]. The two-phase, three-phase, and even multiphase calcium orthophosphates, where different components cannot be separated from each other, are also known [12,13]. In mineralogy, compounds, such as tetracalcium phosphate  $\text{Ca}_4(\text{PO}_4)_2\text{O}$  and oxyapatite  $\text{Ca}_{10}(\text{PO}_4)_6\text{O}$ , which do not precipitate from aqueous solutions, are also recognized. One more group of the calcium orthophosphates is the ion-substituted phosphates, namely, the fluorapatites  $\text{Ca}_{10}(\text{PO}_4)_6\text{F}_2$  and  $\text{Ca}_{10}(\text{PO}_4)_6\text{F}(\text{OH})$  [14], the carbonate-containing apatites [15], the apatites with the addition of the different metals cations [1–3,6–8,12,16].

The known synthesis methods of the calcium orthophosphate are conveniently divided into two groups: the solid-state methods when the mixture of calcium and phosphor precursors with a predetermined ratio Ca/P is exposed to heat treatment and the wet chemical methods when the synthesis is carried out by the chemical precipitation in solutions, the hydrothermal method or the other calcium phosphate hydrolysis. As a rule, the solid-state methods are long term and energy-consuming [17]. The wet chemical synthesis methods do not have these drawbacks, but at the same time, the precipitation method allows them to obtain not all the possible calcium orthophosphates [18]. The necessity for strict control over the precipitation conditions is considered to be a significant drawback of synthesis by the method of the solutions chemical precipitation. Nonobservance of these conditions leads to precipitation of the calcium orthophosphates with deviations from a given stoichiometric composition. The possibility of formation during the precipitation process of the metastable phases and the additional phase transformations of already precipitated calcium orthophosphates complicates significantly the determination of their optimum synthesis conditions [10,11,19–22].

The complexity of the precipitation processes of the calcium orthophosphates is well illustrated by the data of the authors of References [23,24] who found, for example, that the synthesis of  $\text{CaHPO}_4\cdot 2\text{H}_2\text{O}$  by treating of the  $\text{Ca}(\text{OH})_2$  suspension with phosphoric acid at equimolar ratio Ca/P takes place in five stages associated with an intermediate formation of the hydroxyapatite phase  $\text{Ca}_{10}(\text{PO}_4)_6(\text{OH})_2$  at the first stage.

According to References [18,25–28], precipitation of hydroxyapatite upon mixing of calcium salts and phosphate ions, even with a strict stoichiometric ratio  $\text{Ca}/\text{P} = 1.67$ , proceeds through the formation of non-stoichiometric amorphous or calcium-deficient calcium phosphate. Herewith, the chemical composition of the hydroxyapatite surface is not necessarily the same as its volume composition [29].

It may also be noted that the authors of Reference [30] experimentally proved that even relatively small adjustments to chemical precipitation conditions (temperature, aging period, pH) significantly affect the morphological and chemical characteristics of calcium phosphates precipitates. As a consequence, it is necessary to monitor the conditions of the precipitation reaction.

For a more detailed illustration of this conclusion the data on the synthesis conditions for the known calcium orthophosphates are presented in Table 1. Conspicuous is the fact that not only the acidity of the mother solution but also the temperature are considered to be significant factors of such a synthesis according to all the suggested methodologies.

**Table 1.** The calcium orthophosphates, their solubility products ( $K_S$ ) at 25 °C, and the synthesis conditions.

Compound	$-\lg K_S$ [1,7]	Synthesis Conditions
Calcium dihydrogen phosphate monohydrate (Monocalcium phosphate monohydrate) $\text{Ca}(\text{H}_2\text{PO}_4)_2 \cdot \text{H}_2\text{O}$	1.14	Precipitation is carried out at $\text{pH} < 2.0$ and with a molar ratio $\text{Ca}/\text{P} = 0.5$ [1].
Calcium dihydrogen phosphate anhydrous (Monocalcium phosphate anhydrous) $\text{Ca}(\text{H}_2\text{PO}_4)_2$	1.14	It is not precipitated from the aqueous solutions. It is obtained by dehydration of $\text{Ca}(\text{H}_2\text{PO}_4)_2 \cdot \text{H}_2\text{O}$ at a temperature above 100 °C [1].
Calcium hydrogen phosphate dihydrate (dicalcium phosphate dihydrate) $\text{CaHPO}_4 \cdot 2\text{H}_2\text{O}$	6.59	Precipitation should be carried out at a ratio $\text{Ca}/\text{P} = 1.0$ , $\text{pH} = 2.0$ – $6.5$ and at a temperature below 80 °C [12].
Calcium hydrogen phosphate anhydrous (dicalcium phosphate anhydrous) $\text{CaHPO}_4$	6.90	It can be synthesized by the precipitation method from a boiling aqueous solution at ratio $\text{Ca}/\text{P} = 1.0$ and $\text{pH} = 2.0$ – $6.5$ [26,31].
Calcium phosphate tribasic beta ( $\beta$ -tricalcium phosphate) $\beta\text{-Ca}_3(\text{PO}_4)_2$	28.9	It is not precipitated from the aqueous solutions. It is obtained by thermal decomposition of the calcium-deficient hydroxyapatite at a temperature above 750 °C or by the solid-state reaction between $\text{CaHPO}_4$ and $\text{CaO}$ [32]. $\beta\text{-Ca}_3(\text{PO}_4)_2$ can also be obtained by precipitation from ethylene glycol at 150 °C temperature [33,34].
Calcium phosphate tribasic alpha ( $\alpha$ -tricalcium phosphate) $\alpha\text{-Ca}_3(\text{PO}_4)_2$	25.5	It is not precipitated from the aqueous solutions. It is obtained by thermal treatment of $\beta\text{-Ca}_3(\text{PO}_4)_2$ at a temperature above 1125 °C [12].
Amorphous calcium phosphate $\text{Ca}_x\text{H}_y(\text{PO}_4)_z \cdot n\text{H}_2\text{O}$ , $n = 3$ – $4.5$	26–33	It is precipitated at $\text{pH} = 5.0$ – $12.0$ . Ratio $\text{Ca}/\text{P}$ varies in the range of 1.20–2.20. It is considered to be an individual calcium orthophosphate with a variable chemical composition. However, it can also be considered as an amorphous form of the other calcium phosphates [1,35].
Octacalcium bis(hydrogenphosphate) tetrakis(phosphate) pentahydrate (Octacalcium phosphate) $\text{Ca}_8(\text{HPO}_4)_2(\text{PO}_4)_4 \cdot 5\text{H}_2\text{O}$	96.6	It is precipitated at a ratio $\text{Ca}/\text{P} = 1.33$ and $\text{pH} = 5.5$ – $7.0$ [36–39]. It is considered to be an unstable intermediate phase. When aging in solution, it transforms to calcium-deficient hydroxyapatite [38]. It is obtained by simultaneous addition of the calcium salts and phosphoric acid at ratio $\text{Ca}/\text{P} = 1.50$ – $1.67$ into boiling water at $\text{pH}$ of 6.5–9.5 with subsequent suspension boiling over several hours [40,41]. It is also obtained by the hydrolysis of $\alpha\text{-Ca}_3(\text{PO}_4)_2$ [42–44] or amorphous calcium phosphate [45–48].
Calcium-deficient hydroxyapatite $\text{Ca}_{10-x}(\text{HPO}_4)_x(\text{PO}_4)_{6-x}(\text{OH})_{2-x}$ , where $0 < x < 1$ .	85 *	Its precipitation is carried out at a ratio $\text{Ca}/\text{P} = 1.67$ , $\text{pH} = 9.5$ – $12.0$ , and at a temperature of $\sim 90$ °C [18,49–55].
Hydroxyapatite $\text{Ca}_{10}(\text{PO}_4)_6(\text{OH})_2$	116.8 *	

\* The solubility product values of these phosphates are proposed to be corrected as follows (see Section 3.3.):  $\text{p}K_S$  for hydroxyapatite is 155,  $\text{p}K_S$  for Ca-deficient hydroxyapatites is 114–155.

Thus, the study of the chemical precipitation process of the calcium orthophosphates is not a trivial task. The analysis of the data in the literature shows that, as a rule, the authors carried out the calcium phosphates synthesis with molar ratios of  $\text{Ca}/\text{P}$  which were determined by the stoichiometric composition of a target product (see Table 1). The same goes for solubility isotherms of all the calcium orthophosphates described in the literature that was calculated or experimentally studied by dissolving of their stoichiometric composition samples [10,11,19–22]. In our opinion, it should be taken into account that any excess of the calcium ions or phosphate ions in the mother solution compared with the stoichiometric ratio  $\text{Ca}/\text{P}$  in the precipitates will lead to an equilibrium displacement in the dissociation reactions of the precipitated calcium phosphate that, in turn, will lead to its solubility change and, as a result, will change its optimum precipitation. Therefore, theoretical and practical interest is a comprehensive study of the influence of precipitation conditions on the composition of calcium phosphates.

The purpose of this paper was to study the processes of chemical precipitation of the calcium orthophosphates from aqueous solutions depending on their acidity, molar ratio Ca/P, and temperature. In order to achieve such a purpose, the thermodynamic solubility isotherms and concentration solubility isotherms should be estimated for the known calcium orthophosphates and a comparative analysis of the recommended conditions for their chemical precipitation should be made.

## 2. Experimental Methods and Calculations

### 2.1. Calcium Orthophosphates Synthesis

All the reagents used in this study were analytical grade and supplied by Merck (Merck KGaA, Darmstadt, Germany). The  $\text{CaCl}_2$  and  $\text{H}_3\text{PO}_4$  were used as the Ca and P precursors with the Ca/P molar ratio of 0.5–1.67. The KCl was used as an indifferent electrolyte in order to support the constant ionic strength of the solutions.

The calcium phosphate precipitation was carried out by a continuous crystallization at constant supersaturation [52]. The KCl with the concentration of 3 mol/L in the volume of 500 mL was put in a liter flask, and then its pH was corrected to predetermined pH values from 3 to 11 using hydrochloric acid or ammonia solutions. Next, the mixture of the  $\text{CaCl}_2$  and  $\text{H}_3\text{PO}_4$  solutions (prepared with a given Ca/P ratio) and also the ammonia solution with a concentration of 3 mol/L were simultaneously added to the solution using a laboratory peristaltic pipette tip with a dosage amount of 0.05–1 mL/min while continuously mixing the solution by a hand mixer with a rotation speed of 300 rpm.

Automatic support of a given pH level was ensured using an Arduino Uno microcontroller ATmega328P-AU (Arduino Uno, Shenzhen, China) controlled by a computer using the Standard Firmata protocol. The pH measurements were carried out within a pH accuracy of  $\pm 0.05$  using an Adwa AD 8000 pH meter (ADWA, Szeged, Hungary) with silver chloride and glass electrodes. The dosing rate of the reagent solutions was calculated based on the precipitation reactions stoichiometry, and this rate was tested in the preliminary experiments so that the solution pH in the reaction vessel remained at the predetermined level within an accuracy of  $\pm 0.1$  pH during the entire precipitation process.

The obtained precipitates were left in the mother solution at room temperature in the tightly closed flasks for crystallization (so-called aging). In a number of experiments, the suspensions were transferred to a high-pressure Teflon reactor and kept at a temperature of 250 °C for 6 h in order to increase the crystallinity of the precipitates (which made it possible to identify their compositions by the XRD method). The obtained suspensions were filtered under vacuum, washed with small portions of cold distilled water, and dried in a heat chamber at 90–100 °C temperature.

### 2.2. Materials Characterization

The X-ray phase analysis was performed using a diffractometer DRON-2 (Bourestnik JSC, St. Petersburg, Russian Federation) in the monochromatic  $\text{Co-K}\alpha_1$  emission. In order to identify the phase composition under the PCPDFWIN (PCPDFWIN, Newtown Square, PA, USA) database, the diffraction patterns were converted according to  $\text{Cu-K}\alpha_1$  emissions. To analyze diffraction patterns, the Match!2 (Crystal impact, Bonn, Germany) software package was used. It allowed us to make a qualitative (using the PCPDFWIN crystallographic databases) and quantitative (using the iterative Rietveld refinement method) identification of the diffraction patterns.

In order to evaluate the Ca/P ratio, ICP (Inductively Coupled Plasma) analysis was performed by Varian Liberty 200 (Varian Inc., Palo Alto, CA, USA) apparatus.

### 2.3. Determination of Apparent Constants of the Phosphoric Acid Protolytic Dissociation

The potentiometric titration curves of the phosphoric acid solution with the concentration of 0.1 mol/L were studied by a standard solution of the potassium hydroxide at various excesses of the background KCl electrolyte (0.25–5.0 mol/L) in order to determine the influence of the solutions ionic strength on the dissociation constants of the phosphoric acid. Potassium chloride was also

added to the KOH solution in the required amount so that the ionic strength does not change during titration. Measurements were carried out at a room temperature of 15 °C. Calculation of the dissociation constants was carried out according to the following formulas:

$$pK_1 = \left( pH_1 - \frac{1}{2}pK_2 \right) \times 2 \quad (1)$$

$$pK_2 = \left( pH_2 - \frac{1}{2}pK_3 \right) \times 2 \quad (2)$$

$$pK_3 = \left( pH_3 - \frac{1}{2}pK_w - \frac{1}{2} \lg C_{\text{salt}} \right) \times 2 \quad (3)$$

where  $pH_1$ ,  $pH_2$ , and  $pH_3$  are the pH values at the titration endpoints (equivalence points) on the pH titration curves ( $V_{\text{KOH}}$ ) determined by their differentiation;  $pK_w$  is a negative decimal logarithm of the ionic product of water; and  $C_{\text{salt}}$  is the molar concentration of  $K_3PO_4$  salt at the moment the titration endpoint is reached at  $pH_3$ .

When calculating the salt concentration and the solutions ionic strength, it was taken into account the strength correction of electrolytes due to the dilution of the initial acid volume which was taken for titration ( $V_{SH} = V_{H_3PO_4} + V_{KOH}$ ).

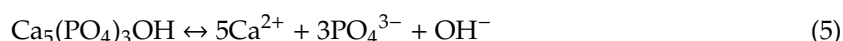
#### 2.4. Calculation of the Solubility Isotherms of the Calcium Orthophosphates

The precipitates solubility was calculated using the following formula for a solubility product of the ionic precipitates, namely:

$$K_s = (xS\beta_i)^x \times (yS\alpha_i)^y \quad (4)$$

where  $S$  is a solubility, mol/L;  $x$ ,  $y$  are stoichiometric coefficients in the dissociation formula;  $\alpha_i$  and  $\beta_i$  are the precipitate anions and cations proportions with an account for the acid dissociation reactions and the stability constants of the cation complexes with phosphate ions and hydroxide ions.

An example of using Formula (4) for calculating a hydroxyapatite solubility is given below:



Upon dissolution of the  $S$  mole of hydroxyapatite after reaching equilibrium of reaction (5), the concentration of all forms of dissolved calcium will be:

$$[Ca^{2+}] + [Ca(OH)^+] + [Ca(OH)_2^0] + [Ca(H_2PO_4)^+] + [Ca(HPO_4)^0] + [Ca(PO_4)^-] = 5S \text{ mol} \quad (6)$$

and the sum of concentrations of all the phosphates forms will be:

$$[PO_4^{3-}] + [HPO_4^{2-}] + [H_2PO_4^-] + [H_3PO_4] + [Ca(H_2PO_4)^+] + [Ca(HPO_4)^0] + [Ca(PO_4)^-] = 3S \text{ mol} \quad (7)$$

The concentration of the  $OH^-$  ions will be determined by a solution pH value (if  $S \ll C_{OH}$ ) or by a hydroxyapatite solubility (if  $S \gg C_{OH}$ ).

The ratios between the phosphates and calcium forms are determined by the coefficients  $\alpha_i$  and  $\beta_i$  which depend on pH value and, in their turn, are determined based on the dissociation constants of the phosphoric acid ( $K_i$ ) and the stability constants of the hydroxide calcium complexes ( $K_i^{CaOH}$ ) and phosphate calcium complexes ( $K_i^{CaP}$ ):

$$\alpha_0 + \alpha_1 + \alpha_2 + \alpha_3 + \alpha_4 + \alpha_5 + \alpha_6 = 1 \quad (8)$$

$$\beta_0 + \beta_1 + \beta_2 + \beta_3 + \beta_4 + \beta_5 = 1 \quad (9)$$

For the case under consideration,  $[PO_4^{-3}] = 3\alpha_3S$  and  $[Ca^{2+}] = 5\beta_0S$ , where:

$$\alpha_3 = \frac{(K_1K_2K_3)}{([H^+]^3 + [H^+]^2K_1 + [H^+]K_1K_2 + K_1K_2K_3) + A}, \quad (10)$$

$$\beta_0 = \frac{1}{(1 + [OH^-]K_1^{CaOH} + [OH^-]^2K_1^{CaOH}K_2^{CaOH} + B)}, \quad (11)$$

$$A = \beta_0C_{Ca}[H^+]^2K_1K_1^{CaP} + \beta_0C_{Ca}[H^+]K_1K_2K_2^{CaP} + \beta_0C_{Ca}K_1K_2K_3K_3^{CaP}, \quad (12)$$

$$B = \alpha_1C_PK_1^{CaP} + \alpha_2C_PK_2^{CaP} + \alpha_3C_PK_3^{CaP}. \quad (13)$$

where  $A$  and  $B$  are parts of the formula for  $\alpha_3$  and  $\beta_0$  which describe the contribution of the calcium phosphate complexes with the phosphate ions;  $C_{Ca}$  and  $C_P$  are the general equilibrium concentration of calcium and phosphates in the solution which are determined by the solubility of the hydroxyapatite:  $C_{Ca} = 5S$  and  $C_P = 3S$ .

Summing up what has been said, according to Formula (4), the hydroxyapatite solubility product can be written as follows:

$$K_s = [Ca^{2+}]^5[PO_4^{3-}]^3[OH^-] = (5\beta_0S)^5(3\alpha_3S)^3(S + C_{OH}) \quad (14)$$

### 3. Results

#### 3.1. The Calcium Orthophosphates Synthesis and the Results of Their Study by the XRD Method

In order to investigate the patterns of the phase formation processes during calcium phosphates precipitation, the calcium phosphates syntheses were carried out with variability of the solution's acidity from 3 to 11 pH and at different molar ratios Ca/P which varied between 0.5–1.67. The synthesis temperature and the precipitate aging period in the mother solution were considered variable factors. The experimental conditions and the results of the study of precipitates by the XRD method are presented in Table 2.

**Table 2.** The conditions of synthesis and aging, phase composition of calcium phosphate precipitates.

Precipitation, pH	Ca/P Molar Ratio	Temperature, °C	Time of Aging, Hours	Crystallization at 250 °C	Phase Composition
3.0	0.5	20	24	–	CaHPO <sub>4</sub> ·2H <sub>2</sub> O
		15	6	–	CaHPO <sub>4</sub> ·2H <sub>2</sub> O
3.8 *	0.5	50	6	–	CaHPO <sub>4</sub>
		90	6	–	CaHPO <sub>4</sub>
4.0	1.5	20	24	+	CaHPO <sub>4</sub>
5.0	1.5	20	24	+	86% of CaHPO <sub>4</sub> , 14% of Ca <sub>10</sub> (PO <sub>4</sub> ) <sub>6</sub> (OH) <sub>2</sub>
6.0	1.5	20	24	+	72% of CaHPO <sub>4</sub> , 28% of Ca <sub>10</sub> (PO <sub>4</sub> ) <sub>6</sub> (OH) <sub>2</sub>
7.0	1.5	20	24	+	52% of CaHPO <sub>4</sub> , 48% of Ca <sub>10</sub> (PO <sub>4</sub> ) <sub>6</sub> (OH) <sub>2</sub>
8.0	1.5	20	24	+	36% of CaHPO <sub>4</sub> , 64% of Ca <sub>10</sub> (PO <sub>4</sub> ) <sub>6</sub> (OH) <sub>2</sub>
8.0	1.0	30	6	–	Calcium-deficient hydroxyapatite, Ca/P = 1.51 ± 0.05
		50	6	–	Calcium-deficient hydroxyapatite, Ca/P = 1.55 ± 0.05
9.0	1.5	20	24	+	30% of CaHPO <sub>4</sub> , 70% of Ca <sub>10</sub> (PO <sub>4</sub> ) <sub>6</sub> (OH) <sub>2</sub>
10.0	1.5	20	24	+	32% of CaHPO <sub>4</sub> , 68% of Ca <sub>10</sub> (PO <sub>4</sub> ) <sub>6</sub> (OH) <sub>2</sub>
11.0	0.5	20	24	–	Calcium-deficient hydroxyapatite, Ca/P = 1.67 ± 0.05

\* Precipitation was carried out in the acetate buffer solution in order to maintain a constant pH during precipitate aging in the mother solution.



### 3.2. Calcium Phosphate Diffraction Pattern Reflexes Shift Effect

Analysis of the diffraction patterns of the  $\text{CaHPO}_4 \cdot 2\text{H}_2\text{O}$  and  $\text{CaHPO}_4$  precipitates obtained at pH 3–6 showed an interesting effect of the reflexes shifting relative to their reference data in the direction of decreasing  $2\theta$  by 0.3–0.45 degrees (Figures 1 and 2). In this case, the degree of such reflexes shifting was not constant but decreased with the increasing of the precipitates' aging period in the mother solutions. It is shown in Figure 3, as an example, several reflexes of dicalcium phosphate dihydrate lattice (in Supplementary Materials).

A similar phenomenon is known in solid-state chemistry and is explained by the crystal cell compression when it forms in the volume of the previously obtained precipitate. The change in interplanar spacings during the aging of the sediment indicates a decrease in such compression and a gradual transition of the sediment structure to its equilibrium state. It should be noted that this effect was established with the reference to the chemical precipitates which were not subjected to additional heat treatment, as was the case with the samples presented in the PCPDFWIN reference book. It is reliably known that during heat treatment of the material with ionic cells, the crystallites continue their growth, and stress in their crystal structure relieves gradually.

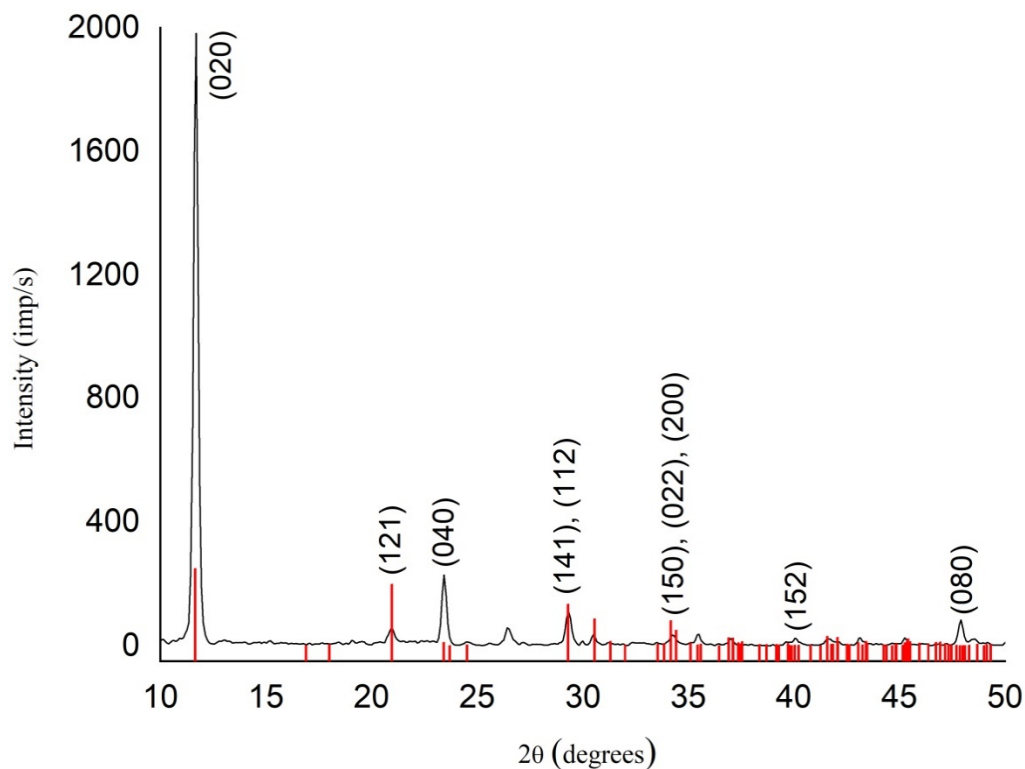


**Figure 1.** The X-ray diffraction pattern of calcium orthophosphate precipitated at pH 3.0, temperature 20 °C, and initial ratio Ca/P = 0.5. The diffraction pattern shifted 0.45 degrees left to match the reference data for dicalcium phosphate dihydrate (PCPDFWIN (PCPDFWIN, Newtown Square, PA, USA) No. 72-0713), which are shown in the figure with the red lines. The additional reflex at 26.4 degrees can be described as an impurity element of dicalcium phosphate anhydrous  $\text{CaHPO}_4$  (No. 77-0128).



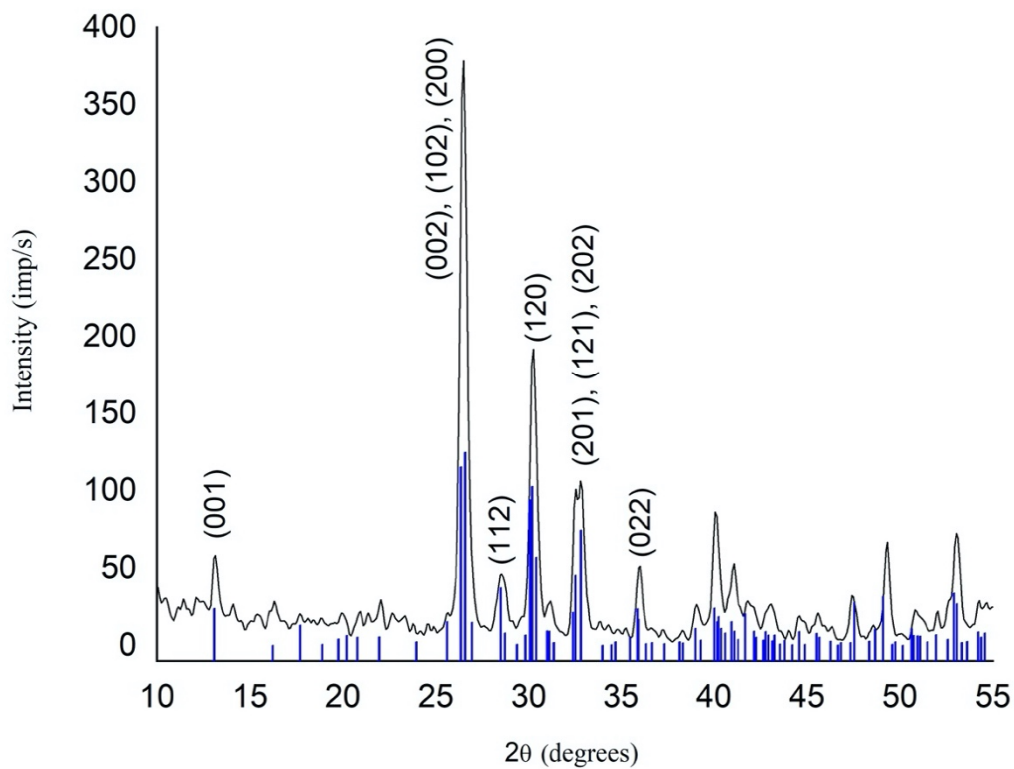


**Figure 2.** The X-ray diffraction pattern of calcium orthophosphate precipitated at pH 3.8, temperature 50 °C, and initial ratio Ca/P = 0.5. The diffraction pattern shifted by 0.45 degrees left to match the reference data for dicalcium phosphate anhydrous (PCPDFWIN No. 77-0128), which are shown in the figure with the blue lines.

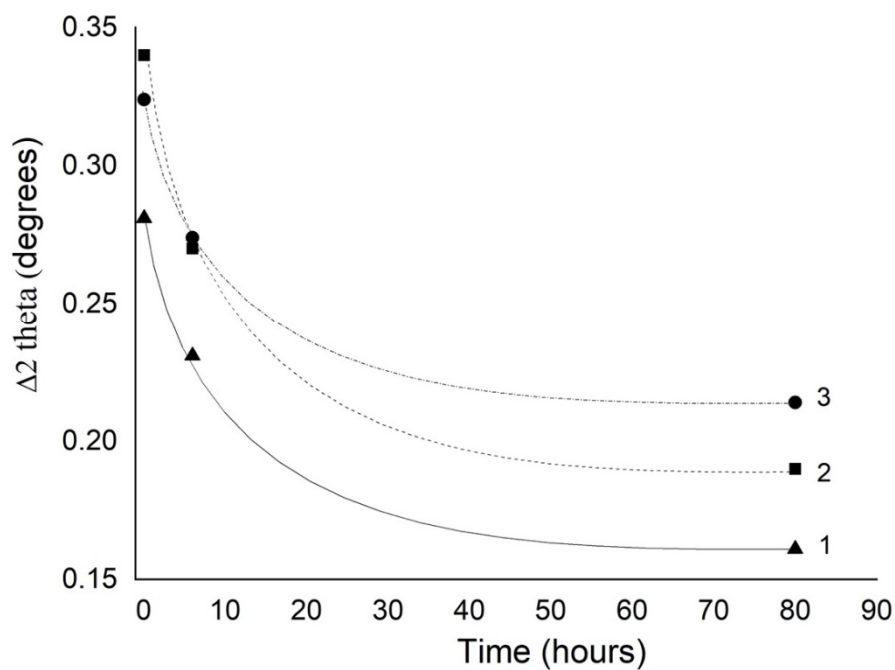


**Figure 3.** The reflexes shifting of the X-ray diffraction pattern of dicalcium phosphate dihydrate when aging in the mother solution: 1—20.95 degrees, 2—11.65 degrees, 3—29.30 degrees. The precipitate was synthesized at pH 3.8, temperature 15 °C, and initial ratio Ca/P = 0.5.

### 3.3. Comparison of the Solubility Products of Calcium Phosphates with Their Chemical Composition

To calculate the solubility isotherms (i.e., the graphs of the dependence of precipitation solubility on the pH of solutions at constant temperature), data on the solubility products ( $K_S$ ) of precipitation are needed. A lot of studies are dedicated to the determination of the precipitates' solubility products and the summary data on their thermodynamic values, found by the constants extrapolating for zero ionic strength of the solutions, are presented in Table 1.

Our attention was drawn to the information that octacalcium phosphate  $\text{Ca}_8(\text{HPO}_4)_2(\text{PO}_4)_4 \cdot 5\text{H}_2\text{O}$  changes into Ca-deficient hydroxyapatite when aging in the mother solution [38]. The solubility products of these orthophosphates are  $2.5 \times 10^{-97}$  and  $\sim 1 \times 10^{-85}$ , respectively (Table 1). Assuming that the solubilities of these phosphates are approximately proportional to their  $K_S$  values, we must conclude that less soluble octacalcium phosphate spontaneously turns into a more soluble Ca-deficient hydroxyapatite. Obviously, such a conclusion contradicts the thermodynamics of equilibrium processes and the solution of such a discrepancy is possible only under the condition that one of the considered  $K_S$  values is determined with an error of at least 12 orders of magnitude.

That is why we made an effort in order to compare the known solubility product values with the calcium orthophosphates compositions. According to the data in Table 1, the solubility products values decrease from top to bottom of this Table, i.e., in the series:  $\text{Ca}(\text{H}_2\text{PO}_4)_2 > \text{CaHPO}_4 > \text{Ca}_3(\text{PO}_4)_2 > \text{Ca}_x\text{H}_y(\text{PO}_4)_z \cdot n\text{H}_2\text{O} > \text{Ca}_{10-x}(\text{HPO}_4)_x(\text{PO}_4)_{6-x}(\text{OH})_{2-x} > \text{Ca}_8(\text{HPO}_4)_2(\text{PO}_4)_4 > \text{Ca}_{10}(\text{PO}_4)_6(\text{OH})_2$ . Conspicuous is the fact that the  $K_S$  values change symbasically due to the number of the calcium cations in the orthophosphate formula. The results of comparing the specific solubility products  $\lg K_S/n(\text{Ca})$  with a molar ratio Ca/P for the known calcium orthophosphates are shown in Figure 4. It was found that there is a linear correlation ( $R^2 = 0.9742$ ) between  $\lg K_S/n(\text{Ca})$  and Ca/P if we exclude the points for hydroxyapatite and its Ca-deficient form from this consideration:

$$\frac{-\lg K_S}{n(\text{Ca})} = -5.0 + 12.26 \frac{n(\text{Ca})}{n(\text{P})} \quad (15)$$

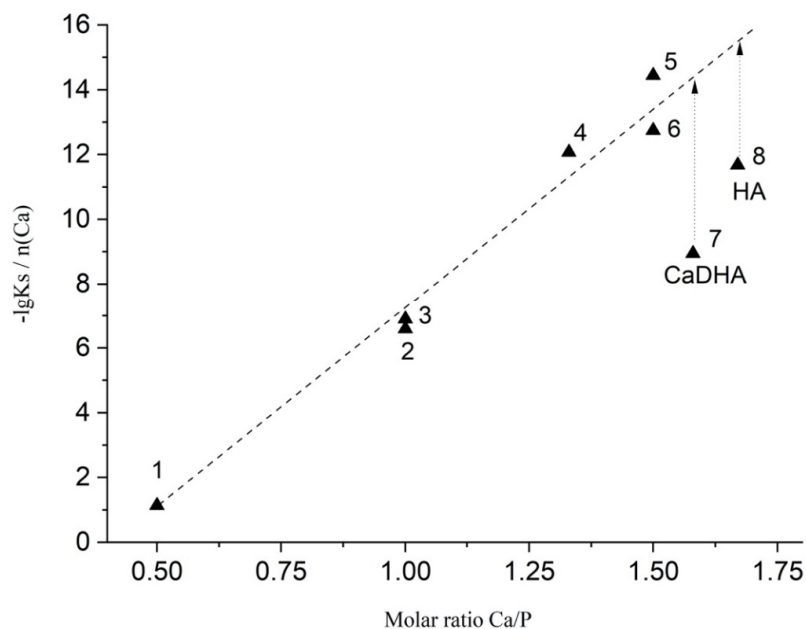


**Figure 4.** Comparison of the specific solubility product values of the calcium orthophosphates (rated per one calcium ion in their formula) with molar ratio Ca/P regarding the following calcium orthophosphates: 1— $\text{Ca}(\text{H}_2\text{PO}_4)_2 \cdot \text{H}_2\text{O}$ ; 2— $\text{CaHPO}_4 \cdot 2\text{H}_2\text{O}$ ; 3— $\text{Ca}_8(\text{HPO}_4)_2(\text{PO}_4)_4 \cdot 5\text{H}_2\text{O}$ ; 4— $\text{Ca}_8(\text{HPO}_4)_2(\text{PO}_4)_4$ ; 5— $\beta\text{-Ca}_2(\text{PO}_4)_3$ ; 6— $\alpha\text{-Ca}_2(\text{PO}_4)_3$ ; 7— $\text{Ca}_{10x}(\text{HPO}_4)_x(\text{PO}_4)_{6-x}(\text{OH})_{2-x}$ , where  $x = 0.5$ ; 8— $\text{Ca}_{10}(\text{PO}_4)_6(\text{OH})_2$ .

Assuming that the solubility product values for hydroxyapatite and its Ca-deficient form are also to have complied with Formula (7), we calculated their solubility isotherms. The results of such calculations under Formula (6) are shown in Figure 5. The hydroxyapatite solubility curve with the more widely accepted  $-\lg K_S$  value of 116.8 under the literature data (Curve 4 in Figure 5) is also shown for reference.

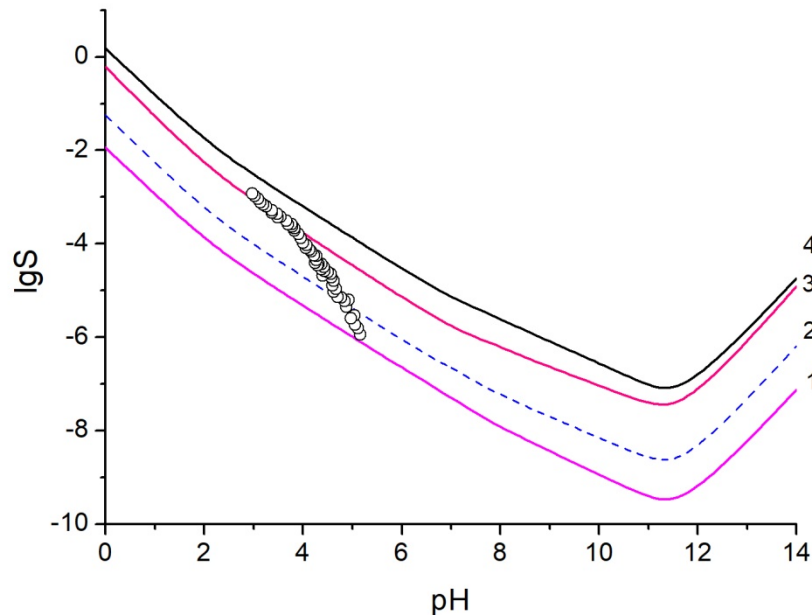


**Figure 5.** The solubility isotherms calculated according to the corrected solubility product values of the following calcium orthophosphates: 1—hydroxyapatite ( $-\lg K_S = 155$ ); 2—Ca-deficient hydroxyapatite with Ca/P of 1.58 ( $-\lg K_S = 136.5$ ); 3—Ca-deficient hydroxyapatite with Ca/P of 1.50 ( $-\lg K_S = 113.8$ ). Curve (4) is plotted for hydroxyapatite with the  $-\lg K_S$  value of 116.8. Points in the figure are given according to the experimental data in Reference [19].

According to Figure 5, the experimental data from Pan and Darvell in Reference [19] are in good agreement with our calculations carried out according to the solubility product values of hydroxyapatite and its Ca-deficient forms which were corrected under Formula (7). Calculations based on the common  $K_S$  value for hydroxyapatite do not make it possible to explain its observed solubility, which pushed the authors of Reference [19] to make a conclusion on the necessity of the  $K_S$  value re-evaluation regarding hydroxyapatite. In their opinion, all solubility calculations are based on simplifications which are only crudely approximate. The problem lies in incongruent dissolution, leading to phase transformations and a lack of detailed solution equilibria.

Pan and Darvell [19] used the method of solid titration when the hydroxyapatite suspension was put into the solution with small portions, and the hydroxyapatite suspension solubility was recorded according to the solution turbidity. They experimentally investigated the precipitates compositions such as Ca/P =  $1.48 \pm 0.05$  at pH of 3.2, Ca/P =  $1.50 \pm 0.05$  at pH of 3.6, Ca/P =  $1.60 \pm 0.05$  at pH of 4.1 [56]. These data show that Pan and Darvell [19] dealt with Ca-deficient hydroxyapatite, for which the Ca/P ratio varies in the range of 1.5–1.67. The solubility zone of the Ca-deficient hydroxyapatites is located between Curves 1 and 3 in Figure 5. Curve 2 is shown as a solubility example of one of the possible Ca-deficient hydroxyapatite forms for which Ca/P is 1.58 ( $\text{Ca}_{10-x}(\text{HPO}_4)_x(\text{PO}_4)_{6x}(\text{OH})_{2x}$ , where  $x = 0.5$ ).

It should be noted that the correction of the solubility products of hydroxyapatite and its Ca-deficient forms in the direction of their decrease allows us to explain the abovementioned fact of the spontaneous conversion of octacalcium phosphate during aging in the mother liquor into Ca-deficient hydroxyapatite. If the  $-\lg K_S$  value for octacalcium phosphate is 96.6, then for Ca-deficient forms of

hydroxyapatite, it now varies in the range 114–155 depending on their composition, i.e., the more soluble octacalcium phosphate should be transformed into the less soluble Ca-deficient hydroxyapatite.

### 3.4. Solubility Isotherms of the Calcium Phosphates at Stoichiometric Ratios Ca/P

There were shown the calculated solubility isotherms regarding the following precipitates  $\text{Ca}(\text{H}_2\text{PO}_4)_2 \cdot \text{H}_2\text{O}$ ,  $\text{CaHPO}_4 \cdot 2\text{H}_2\text{O}$ ,  $\text{CaHPO}_4$ ,  $\text{Ca}_8(\text{HPO}_4)_2(\text{PO}_4)_4 \cdot 5\text{H}_2\text{O}$ ,  $\text{Ca}_9(\text{HPO}_4)(\text{PO}_4)_5(\text{OH})$ , and  $\text{Ca}_{10}(\text{PO}_4)_6(\text{OH})_2$  in Figure 6. The calculation data regarding the solubilities of  $\text{Ca}(\text{OH})_2$  and  $\beta\text{-Ca}_3(\text{PO}_4)_2$ , precipitation of which is considered to be impossible in the system  $\text{Ca}^{2+}\text{-PO}_4^{3-}\text{-H}^+/\text{OH}^-$  due to the fact of their metastable character, were also shown in Figure 6 for comparison. In our calculations, we used the corrected data on the solubility products of hydroxyapatite and its Ca-deficient form  $\text{Ca}_9(\text{HPO}_4)(\text{PO}_4)_5(\text{OH})$ . Similar calculations with the more widely accepted  $K_S$  value, presented in Table 1, show that octacalcium phosphate is the most stable phase until pH is 11, which is contrary to the numerous experimental data [1–12]. According to Figure 6, octacalcium phosphate is a metastable phase after the  $K_S$  values correction, and hydroxyapatite is the least soluble phosphate in the entire range of pH values from 0 to 14.

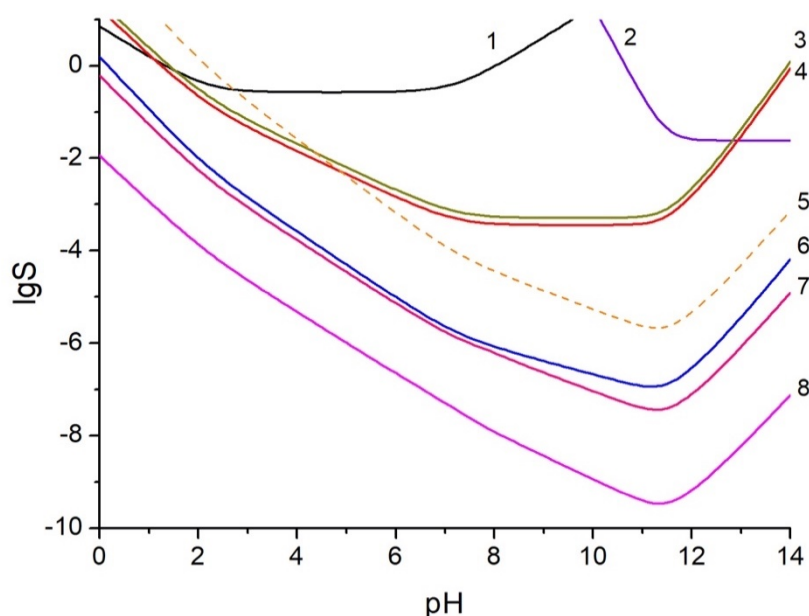


**Figure 6.** The precipitates solubility isotherms regarding  $\text{Ca}(\text{H}_2\text{PO}_4)_2 \cdot \text{H}_2\text{O}$  (1);  $\text{Ca}(\text{OH})_2$  (2);  $\text{CaHPO}_4 \cdot 2\text{H}_2\text{O}$  (3);  $\text{CaHPO}_4$  (4);  $\beta\text{-Ca}_3(\text{PO}_4)_2$  (5);  $\text{Ca}_8(\text{HPO}_4)_2(\text{PO}_4)_4 \cdot 5\text{H}_2\text{O}$  (6); Ca-deficient hydroxyapatite  $\text{Ca}_9(\text{HPO}_4)(\text{PO}_4)_5(\text{OH})$  (7); and  $\text{Ca}_{10}(\text{PO}_4)_6(\text{OH})_2$  (8) at the stoichiometric Ca/P ratios and zero ionic strength.

As noted above, between curves 7 and 8 in Figure 6 there is a family of isotherms for Ca-deficient forms of hydroxyapatite, since according to Formula (7), each such form is characterized by its  $K_S$  value. All these forms are metastable and, when an excess of the calcium ions is added to the solution, they naturally transform into the least soluble hydroxyapatite.

In Figure 6, it should also be distinguished one more family of isotherms for amorphous calcium  $\text{Ca}_x\text{H}_y(\text{PO}_4)_z \cdot n\text{H}_2\text{O}$ , for which the molar ratio Ca/P can vary in the range 1.20–2.20. According to solubility products, their solubility curves should be located slightly higher and lower than the curve 5 for  $\beta\text{-Ca}_3(\text{PO}_4)_2$ . It is likely that this circumstance explains why it is impossible to precipitate the tricalcium phosphates  $\alpha\text{-Ca}_3(\text{PO}_4)_2$  and  $\beta\text{-Ca}_3(\text{PO}_4)_2$  from their aqueous solutions. Instead of these metastable phases the amorphous calcium phosphates are formed, which should transform gradually and naturally into the less soluble forms such as octacalcium phosphate or Ca-deficient hydroxyapatites.

The solubility isotherms in Figure 6 explain very well the natural transformation of  $\text{Ca}_3(\text{PO}_4)_2$  in the aqueous solution into the Ca-deficient hydroxyapatite form which was described in the literature. Obviously, it is possible to disturb the curve course in Figure 6 by changing a solvent chemical nature, that will change the solubility of the involved phosphate precipitates. As a matter of fact, there is factual evidence that it is possible to obtain  $\beta\text{-Ca}_3(\text{PO}_4)_2$  by chemical precipitation using ethylene glycol as a solvent [34,35].

### 3.5. The Solubility Isotherms of the Calcium Phosphates in Solution at a Non-Stoichiometric Ca/P Ratio

As is known, the phase transformations of precipitated calcium orthophosphate during its aging in the mother solution are accompanied by a regular change in the Ca/P ratio not only in the precipitate but also in the volume of the solution. Such changes in the composition of the solution will cause an equilibrium shift in the reactions of hydrolysis or dissociation and, consequently, changes in the solubility of the precipitates. Therefore, when analyzing the solubility isotherms, one should compare not only the solubility of orthophosphate precipitates in water (i.e., for stoichiometric Ca/P ratios) but also their solubility in solutions with an excess of calcium or phosphoric acid salts.

Before considering the calcium orthophosphates solubilities in solutions with a non-stoichiometric Ca/P ratio, it is necessary to clarify the influence patterns of the solution's ionic strength over the equilibrium of dissolution processes. The fact is that the solubility isotherms shown in Figure 6 were calculated using the thermodynamic dissociation constants and solubility products, which were determined at fairly low concentrations of solutions or extrapolated to the zero ionic strength of the solutions. For example, if the precipitation is carried out at an excessive amount of calcium chloride with the concentration of 1 mol/L, then the solution ionic strength can be calculated as follows:

$$I = \frac{1}{2} \sum (C_i z_i^2) = \frac{1}{2} (1 \times (+2)^2 + 2 \times (-1)^2) = 3 \quad (16)$$

where  $C_i$  is an ion concentration;  $z_i$ —is an ion charge.

It is clear that the phosphates synthesis with the infinite dilution solutions is inappropriate for practical reasons. That is why it is of strong interest to consider the precipitates solubility isotherms at high ionic strengths when the precipitation reactions are carried out using the solutions of the calcium and phosphorus precursors with a relatively high concentration.

The values of the ion activity coefficients when changing the ionic strength in the range from 0 to 1 are well known. The nature of the electrolyte should be taken into account when calculating the activity coefficients at higher values of the ionic strengths. Therefore, to assess the degree of influence of high ionic forces on equilibrium constants, we did not carry out calculations according to the Debye–Hückel theory of strong electrolytes, but experimentally determined the values of dissociation constants in the range of ionic forces from 0.3 to 5. To this purpose, there were carried out potentiometric titration of solutions of phosphoric acid amid the excess of potassium chloride. The apparent constants of a protolytic dissociation of the phosphoric acid were calculated using the pH values at the equivalence points on the titration curves under the Formulas (1)–(3). The calculation results are presented in Figure 7.

It was found that all three constants are subject to change with an increase of the ionic strength. Apparently, the complexity of their changes is connected with a modification of the composition and structure of the hydrated shells around the ions of  $\text{H}_2\text{PO}_4^-$ ,  $\text{HPO}_4^{2-}$  and  $\text{PO}_4^{-3}$ . These ions cannot be simulated by the point charges, as it is allowed under the Debye–Hueckel theory. Due to the fact that their negative charges are unevenly allocated around the oxygen atoms, each of these ions creates its specific hydrated shell, the structure of which should vary with an increase of the counterions quantity in the solution—which are potassium ions.

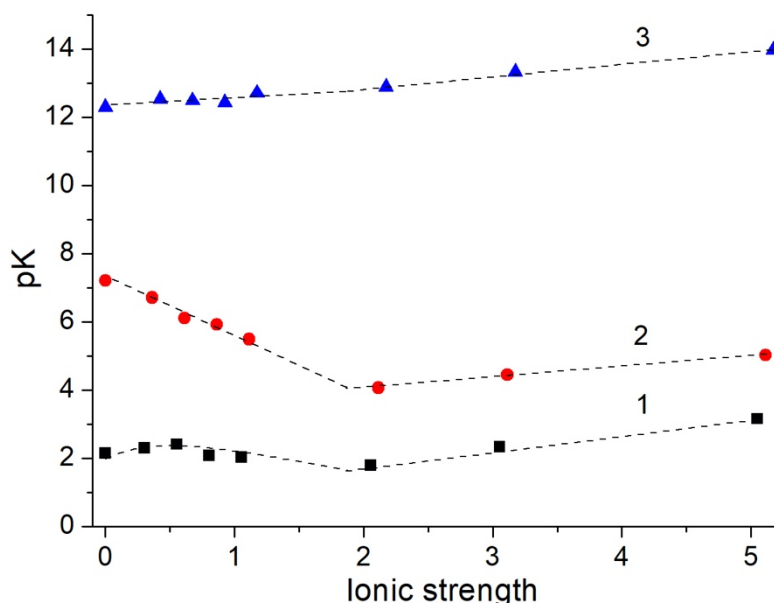


**Figure 7.** The dependence between the apparent constants of a proteolytic dissociation of the phosphoric acid and the solutions ionic strength: 1— $pK_1$ ; 2— $pK_2$ ; 3— $pK_3$ . The KCl solution with a concentration of 0.25–5.0 mol/L was used as the background electrolyte.

We calculated the solubility isotherms for the calcium orthophosphates at the stoichiometric ratios Ca/P in the KCl solution with the concentration of 3 mol/L and in the  $\text{CaCl}_2$  solution with the concentration of 1 mol/L using the found dissociation constants of the phosphoric acid at the ionic strength of 3 ( $K_1 = 5.00 \times 10^{-3}$ ;  $K_2 = 3.98 \times 10^{-5}$ ,  $K_3 = 7.94 \times 10^{-14}$ ) (Figure 8).

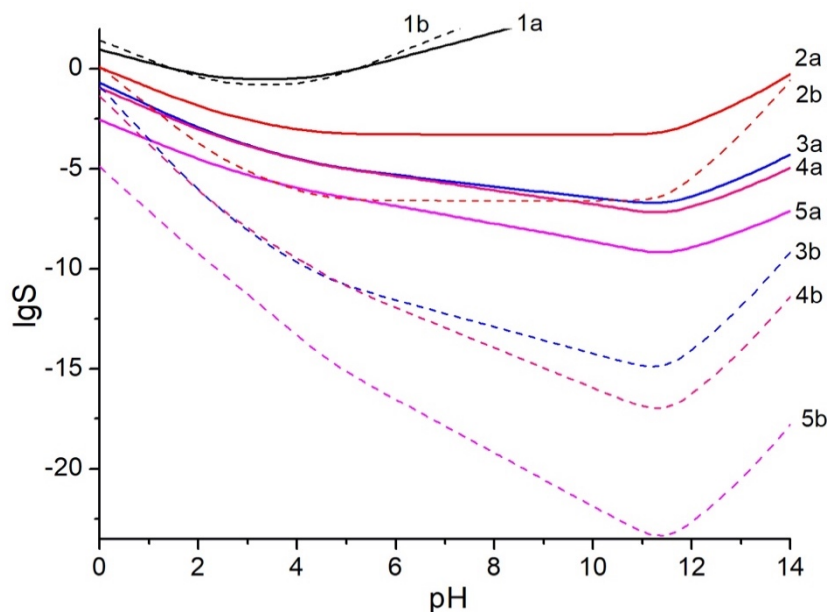


**Figure 8.** The solubility isothermal of the following precipitates:  $\text{Ca}(\text{H}_2\text{PO}_4)_2 \cdot \text{H}_2\text{O}$  (1a, 1b);  $\text{CaHPO}_4 \cdot 2\text{H}_2\text{O}$  (2a, 2b);  $\text{Ca}_8(\text{HPO}_4)_2(\text{PO}_4)_4 \cdot 5\text{H}_2\text{O}$  (3a, 3b); Ca-deficient hydroxyapatite  $\text{Ca}_{10x}(\text{HPO}_4)_x(\text{PO}_4)_{6-x}(\text{OH})_{2-x}$ , ( $x = 1$ ) (4a, 4b); and  $\text{Ca}_{10}(\text{PO}_4)_6(\text{OH})_2$  (5a, 5b) in the KCl solution with the concentration of 3 mol/L and in the  $\text{CaCl}_2$  solution with the concentration of 1 mol/L.

As expected, the addition of excess calcium ions to the solutions sharply reduced the solubility of all phosphates (dashed lines in Figure 8), which is due to the shift in the equilibrium of the dissolution reactions towards the starting reagents. The excess amount of phosphate ions had the same effect.



However, the placing sequence of the solubility isotherms of all the studied phosphates did not change. The stoichiometric hydroxyapatite was still the least soluble phase at any solution composition.

A comparison of the data in Figures 6 and 8 (see the solid lines in Figure 8) shows that the phosphates solubilities at the isotherm's low points were almost the same when the ionic strength was increased to the level of three. Only for calcium dihydrogen phosphate did the pH range of the lowest solubility sharply decrease, while for calcium hydrogen phosphate, on the contrary, it increased. For all other phosphates, the nature of the dependence of the solubility on the pH of the solutions remained practically unchanged.

#### 4. Discussion and Conclusions

The conducted experiments on precipitation of the calcium phosphates (Table 2) showed the substantial influence of the acidity of the mother solution and the temperature over their phase composition. If in acidic solutions at room temperature  $\text{CaHPO}_4 \cdot 2\text{H}_2\text{O}$  is formed, then anhydrous  $\text{CaHPO}_4$  is formed instead of crystalline hydrate during precipitation at 50 °C and higher. The transition of hydrated dicalcium phosphate to the dehydrated form was observed in all cases after maintaining aqueous suspensions at 250 °C. The phenomenon of  $\text{CaHPO}_4 \cdot 2\text{H}_2\text{O}$  dehydration directly in the mother solution has already been described in the literature [26,31].

In composition of the precipitates obtained at  $\text{pH} > 4$  and kept in the mother solutions at 250 °C, the presence of hydroxyapatite was established in addition to dicalcium phosphate. It was found that the ratio of  $\text{CaHPO}_4$  and  $\text{Ca}_{10}(\text{PO}_4)_6(\text{OH})_2$  in such precipitates naturally increases with increasing pH, which indicates the fact that the rate of such transformation depends on the pH of the mother liquor or, more precisely, on the concentration of hydroxide ions which should integrate into the hydroxyapatite crystal lattice. The lower the OH ions concentration in solution, the slower the growth of  $\text{Ca}_{10}(\text{PO}_4)_6(\text{OH})_2$  phase.

It should be noted that the precipitation of the dicalcium phosphate with hydroxyapatite is well known. In the works of References [25–27], the simultaneous precipitation of the dicalcium phosphate with hydroxyapatite was observed even without such high temperature, but only at 37 °C after 24 h of aging in the mother solution with pH of 7.4. The authors of Reference [28] proved the presence of the mixture of the dicalcium phosphate and hydroxyapatite after 1 h of aging of the precipitate under the same experimental conditions.

Unfortunately, we could not manage to reliably prove the presence of mixture of the dicalcium phosphate and hydroxyapatite in the compositions of the precipitates which were obtained at a pH of 8 and were not under heat treatment at 250 °C (Table 2). The chemical analysis of their composition showed that the Ca/P ratios varied in the range of  $(1.51\text{--}1.61) \pm 0.05$ ; this can be explained either as the mixture of the dicalcium phosphate (Ca/P = 1) and hydroxyapatite (Ca/P = 1.67), or as the Ca-deficient forms of hydroxyapatite (Ca/P = 1.5–1.67). The precipitate with the composition Ca/P of  $1.67 \pm 0.05$  was obtained only at a pH of 11. However, the observed difference between the position of its main reflexes and the reference data for hydroxyapatite shows that the Ca-deficient form of hydroxyapatite was formed more likely than the hydroxyapatite phase.

Another interesting pattern in analysis of the data in Table 2 is that the phase compositions of the calcium phosphate precipitates are not dependent on a given molar ratio Ca/P. For example, there were obtained the precipitates of not  $\text{Ca}(\text{H}_2\text{PO}_4)_2 \cdot \text{H}_2\text{O}$  (for which Ca/P is 0.5) but  $\text{CaHPO}_4 \cdot 2\text{H}_2\text{O}$  and  $\text{CaHPO}_4$  (for which Ca/P is 1) during precipitation with an initial molar ratio Ca/P equal to 0.5 in the solutions with pH 3–4.

The fact of a difference between the Ca/P ratios in the mother solutions and in the precipitates obtained from these solutions have been repeatedly noted in the literature. A large number of examples of the similar patterns can be found in the works of Füredi–Milhofer et al. [25–27]. By now, such patterns did not get an explanation. For example, the authors of Reference [21] carried out the phosphate precipitation at the initial ratio Ca/P of 1:1 and at pH of 10, and they obtained the precipitates with Ca/P ratio of 1.5. They explained this surprising mismatch by the hydrolysis of  $\text{CaHPO}_4$  when it



was washed with large amounts of water. This conclusion seems to be hardly probable because pH changing from 10 to neutral values is aligned not with  $\text{PO}_4^{3-}$  ions release but with their fixation into  $\text{HPO}_4^{2-}$  hydrogen phosphates. At the same time, these ions are being continuously removed from the solution during washing, and that initiates the precipitate dissolution process and not hydrolysis. In our opinion, the results of the authors of Reference [21] show that the formation of Ca-deficient hydroxyapatite with Ca/P = 1.5 is possible when mixing solutions of calcium salts and phosphoric acid with Ca/P = 1.0. We also obtained the similar results (see the experiment at pH of 8 in Table 2).

At present, it has been reliably proven that during the precipitation of phosphates even under ideal conditions, i.e., with a strict stoichiometric Ca/P ratio, precipitates of non-stoichiometric composition are formed, which is explained by the formation of such precursor phases as amorphous or Ca-deficient hydroxyapatite [1,7,25–28]. In our opinion, this conclusion may be expressed in the following way: molar ratio Ca/P in the mother solution only slightly determines the composition of calcium phosphate sediments. When setting molar ratio Ca/P, many authors are oblivious to the fact that sediment formation takes place under conditions of a significant excess of one or the other reagent depending on an order of precursor solutions mixing. Particularly strongly, the deposition order affects the composition of precipitates of variable composition which is calcium phosphates. Only when using continuous precipitation while maintaining a constant ratio of the precursors of synthesis, secondary precipitate reactions with excess reagent are leveled [57].

In our opinion, the ratio of the amount of the calcium salts and the phosphoric acid in the reaction solution does not have any substantial influence over the composition of the precipitates until the conditions are created for the phase transitions of their metastable phases to more stable ones.

According to the modern concepts, transformations of the metastable precipitate forms into the states which are more favorable from the thermodynamic point of view, are kinetically blocked due to the existence of the energy barrier in the transformation process of their crystal cell. It is obvious that the temperature increase is necessary for overcoming this activation barrier. This conclusion is well supported by the experimental data. For example, it is known, that Ca-deficient hydroxyapatite can be obtained by adding the calcium salts and phosphoric acid at the ratio Ca/P of 1.50–1.67 into the boiling water at pH of 6.5–9.5 with subsequent suspension boiling during several hours [40,41]. The stoichiometric hydroxyapatite is synthesized in a similar way: it is precipitated at  $\sim 90$  °C maintaining the Ca/P ratio of 1.67 and pH of 9.5–12.0 [49–55].

It is convenient to carry out the direction of the phase transitions of the metastable phases into the more stable phases using the solubility isotherms of the calcium phosphates (Figures 6 and 8). Obviously, the concentration of the calcium ions and phosphoric acid in the mother solution will change from top to bottom during the precipitation. The spontaneous reverse transition (from bottom to top) is thermodynamically forbidden, because it will require an increase in the Gibbs energy of the system instead of its decrease. That is why the data found in the literature (e.g., [23,24]) on possibility of the formation of the dicalcium phosphate or octacalcium phosphate (isotherms 3 and 6 in Figure 6) from the pre-precipitated Ca-deficient hydroxyapatite (group of isotherms between curves 7 and 8 in Figure 6) or hydroxyapatite (isotherm 8 in Figure 6) are doubtful and require a more careful analysis.

Füredi-Milhofer et al. [25–28] used precipitation diagrams instead of solubility isotherms, and they plotted these diagrams in the axis of coordinates for the concentrations of the phosphate ions and calcium ions at a constant pH. The excess amount of the value of the concentrations (activities) product of these ions over the value of the solubility product of the calcium phosphate precipitates is the degree of saturation of the mother solution. As is known, the degree of saturation determines the speed of both the stage of nucleation and the stage of growth of these nucleating seeds, i.e., the precipitation diagrams are conveniently used in studying of the kinetics of the chemical precipitation process in contrast to the equilibrium solubility isotherms. Obviously, various calcium phosphates can coexist in solution at high degrees of saturation, and formation of these various calcium phosphates can be described by the mechanism of simultaneous nucleation of the several phases [7,28] without using the hypothesis of phase transitions of the metastable phases to more stable phases. However, if we consider

the precipitate in the mother solution as the mixture of, for example, the dicalcium phosphate and hydroxyapatite in the equilibrium state, then it is not clear why the more soluble dicalcium phosphate does not completely convert to hydroxyapatite. The solution of this problem requires a thorough study of the kinetics of such phase transition in order to reveal the fact and reasons for the kinetic inhibition of such process.

In conclusion, in this article we used the solubility isotherms of hydroxyapatite and its Ca-deficient forms, and these solubility isotherms were calculated using the updated values of their solubility products. It is obvious that the found correlation between the specific solubility products and molar ratio Ca/P needs a theoretical justification. As is known, the solubility product is an equilibrium constant for a dissolution process of the slightly soluble substance, recording which the solid phase activity is taken equal to unity. In chemical thermodynamics any equilibrium constant can be expressed through a change in the standard Gibbs free energy, as follows:

$$\Delta G_{Diss}^0 = -RT \ln K_s = -RT \ln (a_{Kat})^x (a_{An})^y \quad (17)$$

where  $\Delta G_{Diss}^0$ —is Gibbs energy change during the dissolution of a slightly-soluble substance;  $a_{Kat}$  and  $a_{An}$ —are activities of the precipitates cations and anions.

Considering a dissolution as a process of breaking of the interionic bonds in a solid substance and the intermolecular bonds in a solvent, associated with the process of formation of the new bonds at ions solvation, the following formula can be written down for  $\Delta G_{Diss}^0$ :

$$\Delta G_{Diss}^0 = \Delta G_{Solv}^0 - \Delta G_{Cryst.cell}^0 - \Delta G_{Cav}^0 \quad (18)$$

where  $\Delta G_{Solv}^0$  is solvation energy of ionic precipitates cations and anions;  $\Delta G_{Cryst.cell}^0$  is a crystal cell energy;  $\Delta G_{Cav}^0$  is an energy of a cavity formation in solvent [58,59].

Let us write the solvation energy as the sum of two components—the cations solvation energy and the anions solvation energy, taken separately, and it should be taken into account that due to a difference between the cations and anions sizes, as a rule,  $\Delta G_{Solv.Kat}^0 \gg \Delta G_{Solv.An}^0$ . That is why the formula for  $\Delta G_{Solv}^0$  can be expressed as follows:

$$\Delta G_{Solv}^0 = x\Delta G_{Solv.Kat}^0 + y\Delta G_{Solv.An}^0 \approx x\Delta G_{Solv.Kat}^0 \quad (19)$$

where  $x$  and  $y$  are the cations and anions quantities in a formula for a solid substance.

The energy of a cavity formation in solvent can be calculated as an energy of the solvent microscopic tension on cavity surface through the following formula:

$$\Delta G_{Cav}^0 = \gamma_{micr} F N_A \quad (20)$$

where  $\gamma_{micr}$  is a microscopic surface tension;  $N_A$  is Avogadro's number;  $F$  is a cavity surface area, which is usually calculated based on the effective ionic radius increased by a water molecule radius.

The value of a water microscopic surface tension is  $3 \cdot 10^{-23}$  J/A<sup>2</sup> [60], which allows us to neglect the contribution of  $\Delta G_{Cav}^0$  to the formula (9) in comparison with its other components in order to simplify this theoretical consideration regarding a dissolution process.

An approximation of a discrete (microscopic) model for solid substances with an ion crystal cell, electrostatic energy of one ion is determined as a product of the two following values: this ion charge and potential of the electric field created by the charges of all the other ions of this crystal cell, that can be expressed as follows:

$$E_{el,i} = z_i e V_i, \quad (21)$$

where  $z_i$  is a charge value of one ion;  $e$  is an electron charge;  $V_i$  is an electric field potential.

Madelung constant is used in order to determine the electric potential value for all the ions of the cell under the following formula:

$$V_i = \frac{e}{4\pi\epsilon_0 r_0} \sum \frac{z_i r_0}{r_{ij}} = \frac{e}{4\pi\epsilon_0 r_0} M \quad (22)$$

where  $r_{ij}$  is a distance between the  $i$ -th and  $j$ -th ions;  $r_0$ —is a distance between the nearest neighboring ions in a crystal cell;  $M$  is Madelung constant of the  $i$ -th ion.

If in Madelung constant we select its  $M_0$  part, which exclusively depends on a cell geometric structure, then we can write down the following formula:

$$M = z_{Kat} z_{An} M_0 \sum n \quad (23)$$

where  $z_{Kat}$  and  $z_{An}$ —are the values of cation and anion charges;  $n$ —is the ions quantity in the following substance formula:  $\sum n = x + y$ , where  $x$  and  $y$ —are the stoichiometric coefficients in a substance formula.

If we combine formulas (12)–(14) and add the Avogadro's number in order to apply the formula to 1 mol of a substance, then we have the following formula:

$$E_{el} = (x + y) \frac{z_{Kat} z_{An} e^2 N_A M_0}{4\pi\epsilon_0 r_0} \quad (24)$$

Formula (15) reflects only one component of an interionic interaction in a solid substance, but this formula is sufficient to describe the value of  $\Delta G_{Cryst.cell}^0$  in the formula (9).

Summing up what has been said, the general formula for  $\Delta G_{Diss}^0$  can be written as follows:

$$\Delta G_{Diss}^0 \approx x \Delta G_{Solv.Kat}^0 - (x + y) \frac{z_{Kat} z_{An} e^2 N_A M_0}{4\pi\epsilon_0 r_0} \quad (25)$$

According to this formula, a linear dependence should exist between the standard Gibbs energy of a dissolution process and the ions quantity in its formula ( $x + y$ ). Such dependence is known in the literature, namely: the larger a sum ( $x + y$ ) in a calcium orthophosphate formula, the less its solubility product [1], see Figure 5. For example, hydroxyapatite, for which ( $x + y$ ) = 18, is the least soluble in the following substances list:  $\text{Ca}(\text{H}_2\text{PO}_4)_2$ ,  $\text{CaHPO}_4$ ,  $\text{Ca}_3(\text{PO}_4)_2$ ,  $\text{Ca}_8(\text{HPO}_4)_2(\text{PO}_4)_4$  and  $\text{Ca}_{10}(\text{PO}_4)_6(\text{OH})_2$ .

In order to explain the correlation between the specific solubility product and a molar ratio Ca/P shown in Figure 4, we should decompose the sum ( $x + y$ ) in a Taylor series, i.e., into an infinite sum of power functions:

$$x + y = \frac{x}{b_0} + \frac{x^2}{b_1 y} + \frac{x^3}{b_2 y^2} + \frac{x^4}{b_3 y^3} + \dots, \quad (26)$$

where  $b_i$  are the series coefficients that determine its convergence.

Such expansion is reasonable to subject to the condition that a sum ( $x + y$ ) is a function that continuously changes during the calcium phosphates precipitation. The value of  $x$  (cations quantity) varies from 0 to 10, and the value of  $y$  (anions quantity) varies from 0 to 8 in this example. Despite the fact that only some certain Ca/P ratios are thermodynamically stable (for example 0.5, 1.0, 1.33, 1.5, and 1.67), it is possible that the precipitates with other compounds can also be formed. For example, the existence of the Ca-deficient hydroxyapatites, for which a molar ratio Ca/P varies in the range of 1.5–1.67, has been experimentally proved. From this point of view, it can also be explained the existence of a special class of the amorphous calcium phosphates  $\text{Ca}_x\text{H}_y(\text{PO}_4)_z \cdot n\text{H}_2\text{O}$ , for which a molar ratio Ca/P varies in the range of 1.20–2.20. Thus, it is obvious that Formula (17) is reasonable not only for some specific compounds but for the entirety of the precipitates in the system  $\text{Ca}^{2+}-\text{PO}_4^{3-}-\text{H}^+/\text{OH}^-$ .

Using only the first two terms of the series (17) for simplicity, Formula (16) can be rewritten using formula (8) as follows:

$$-RT \ln K_s \approx x \Delta G_{Solv.Kat}^0 - \left( \frac{x}{b_0} + \frac{x^2}{b_1 y} \right) \frac{z_{Kat} z_{An} e^2 N_A M_0}{4\pi \epsilon_0 r_0}, \quad (27)$$

If we open the brackets and insert the conventional values ( $A$  and  $B$ ) for all the constants, then we will have the following formula:

$$\frac{\ln K_s}{x} \approx A + \frac{x}{y} B \quad (28)$$

which explains fairly well a linear correlation shown in Figure 4 if the ratio of the stoichiometric coefficients  $x$  and  $y$  is expressed in terms of a molar ratio Ca/P.

Thus, a correlation between the specific values of solubility products of the calcium orthophosphates and their molar ratio Ca/P can be explained in terms of the well-known models with a clear physical meaning. That is why this correlation can be used for a prognosis of the  $K_s$  values. Obviously, such prognosis shows some inaccuracy, because several simplifications were admitted at a derivation of Formula (19) and Madelung constant is not the same for the calcium phosphates with different types of the crystal cells. However, a relatively large degree of the  $K_s$  values deviation from the found correlation for hydroxyapatite and its Ca-deficient forms should be interpreted as erroneous data that need to be re-evaluated [19,56].

**Supplementary Materials:** The following are available online at <http://www.mdpi.com/2227-9717/8/9/1009/s1>.

**Author Contributions:** Conceptualization, M.V.N. and K.V.V.; methodology, M.V.N.; software, V.D.M.; validation, M.V.N.; investigation, K.V.V. and V.D.M.; resources, M.V.N.; writing—original draft preparation, M.V.N., K.V.V. and V.D.M.; writing—review and editing, A.K. and B.L.; visualization, K.V.V.; supervision, B.L.; project administration, A.K.; funding acquisition, B.L. All authors have read and agreed to the published version of the manuscript.

**Funding:** The work was supported by R&D project 24/200490 of the Ukrainian State University of Chemical Technology.

**Acknowledgments:** M.V.N. is grateful to Victor G. Vereschak for the provided samples of hydroxyapatite as well as to Yhor M. Ryshchenko for helping with preparing a phosphate technologies literary review. A.K. and B.L. acknowledge financial support from the Slovenian Research Agency (research core funding No. P2-0152).

**Conflicts of Interest:** The authors declare no conflict of interest.

## References

1. Dorozhkin, S.V. Calcium orthophosphates (CaPO<sub>4</sub>): Occurrence and properties. *Prog. Biomater.* **2015**, *5*, 9–70. [[CrossRef](#)] [[PubMed](#)]
2. Dorozhkin, S.V. Calcium Orthophosphate-Containing Biocomposites and Hybrid Biomaterials for Biomedical Applications. *J. Funct. Biomater.* **2015**, *6*, 708–832. [[CrossRef](#)] [[PubMed](#)]
3. Dorozhkin, S.V. Calcium Orthophosphate-Based Bioceramics. *Materials* **2013**, *6*, 3840–3942. [[CrossRef](#)] [[PubMed](#)]
4. Ślósarczyk, A.; Czechowska, J.; Cichoń, E.; Zima, A. New Hybrid Bioactive Composites for Bone Substitution. *Processes* **2020**, *8*, 335. [[CrossRef](#)]
5. Lett, J.A.; Sagadevana, S.; Prabhakar, J.J.; Hamizi, N.A.; Badruddin, I.A.; Johan, M.R.; Ab Rahman, M.; Wahab, Y.A.; Khan, T.Y.; Kamangar, S. Drug Leaching Properties of Vancomycin Loaded Mesoporous Hydroxyapatite as Bone Substitutes. *Processes* **2019**, *7*, 826. [[CrossRef](#)]
6. Dorozhkin, S.V. Nanodimensional and Nanocrystalline Apatites and Other Calcium Orthophosphates in Biomedical Engineering, Biology and Medicine. *Materials* **2009**, *2*, 1975–2045. [[CrossRef](#)]
7. Wang, L.; Nancollas, G.H. Calcium Orthophosphates: Crystallization and Dissolution. *Chem. Rev.* **2008**, *108*, 4628–4669. [[CrossRef](#)]
8. Omelon, S.J.; Grynpas, M.D. Relationships between Polyphosphate Chemistry, Biochemistry and Apatite Biomineralization. *Chem. Rev.* **2008**, *108*, 4694–4715. [[CrossRef](#)]

9. Clark, N.A. The System  $P_2O_5$ -CaO- $H_2O$  and the Recrystallization of Monocalcium Phosphate. *J. Phys. Chem.* **1931**, *35*, 1232–1238. [[CrossRef](#)]
10. Brown, P.W. Phase Relationships in the Ternary System CaO- $P_2O_5$ - $H_2O$  at 25 °C. *J. Am. Ceram. Soc.* **1992**, *75*, 17–22. [[CrossRef](#)]
11. Martin, R.I.; Brown, P.W. Phase Equilibria among Acid Calcium Phosphates. *J. Am. Ceram. Soc.* **2005**, *80*, 1263–1266. [[CrossRef](#)]
12. Dorozhkin, S.V. Dissolution mechanism of calcium apatites in acids: A review of literature. *World J. Methodol.* **2012**, *2*, 1–17. [[CrossRef](#)] [[PubMed](#)]
13. Nakano, T.; Kaibara, K.; Umakoshi, Y.; Imazato, S.; Ogata, K.; Ehara, A.; Ebisu, S.; Okazaki, M. Change in Microstructure and Solubility Improvement of HAp Ceramics by Heat-Treatment in a Vacuum. *Mater. Trans.* **2002**, *43*, 3105–3111. [[CrossRef](#)]
14. Pajor, K.; Pajchel, L.; Kolmas, J. Hydroxyapatite and Fluorapatite in Conservative Dentistry and Oral Implantology—A Review. *Materials* **2019**, *12*, 2683. [[CrossRef](#)] [[PubMed](#)]
15. Siddiqui, H.; Pickering, K.; Mucalo, M.R. A Review on the Use of Hydroxyapatite-Carbonaceous Structure Composites in Bone Replacement Materials for Strengthening Purposes. *Materials* **2018**, *11*, 1813. [[CrossRef](#)]
16. Lin, R.; Ding, Y.-J. A Review on the Synthesis and Applications of Mesostructured Transition Metal Phosphates. *Materials* **2013**, *6*, 217–243. [[CrossRef](#)]
17. Dorozhkin, S.V. Calcium Orthophosphates in Nature, Biology and Medicine. *Materials* **2009**, *2*, 399–498. [[CrossRef](#)]
18. El Briak-BenAbdeslam, H.; Ginebra, M.P.; Vert, M.; Boudeville, P. Wet or dry mechanochemical synthesis of calcium phosphates? Influence of the water content on DCPD-CaO reaction kinetics. *Acta Biomater.* **2008**, *4*, 378–386. [[CrossRef](#)]
19. Pan, H.-B.; Darvell, B.W. Calcium Phosphate Solubility: The Need for Re-Evaluation. *Cryst. Growth Des.* **2009**, *9*, 639–645. [[CrossRef](#)]
20. Piazza, R.D.; Pelizaro, T.A.; Rodríguez-Chanfrau, J.E.; La Serna, A.A.; Veranes-Pantoja, Y.; Guastaldi, A.C. Calcium phosphates nanoparticles: The effect of freeze-drying on particle size reduction. *Mater. Chem. Phys.* **2020**, *239*, 122004. [[CrossRef](#)]
21. Zyman, Z.; Goncharenko, A.; Khavroniuk, O.; Rokhmistrov, D. Crystallization of metastable and stable phases from hydrolyzed by rinsing precipitated amorphous calcium phosphates with a given Ca/P ratio of 1:1. *J. Cryst. Growth* **2020**, *535*, 125547. [[CrossRef](#)]
22. Gregory, T.M.; Moreno, E.C.; Patel, J.M.; Brown, W.E. Solubility of  $\beta$ - $Ca_3(PO_4)_2$  in the System Ca(OH) $_2$ - $H_3PO_4$ - $H_2O$  at 5, 15, 25, and 37 °C. *J. Res. Natl. Bur. Stand. Sect. A Phys. Chem.* **1974**, *78*, 667–674. [[CrossRef](#)] [[PubMed](#)]
23. Ferreira, A.; Oliveira, C.; Rocha, F. The different phases in the precipitation of dicalcium phosphate dihydrate. *J. Cryst. Growth* **2003**, *252*, 599–611. [[CrossRef](#)]
24. Oliveira, C.; Ferreira, A.; Rocha, F. Dicalcium Phosphate Dihydrate Precipitation. *Chem. Eng. Res. Des.* **2007**, *85*, 1655–1661. [[CrossRef](#)]
25. Füredi-Milhofer, H.; Oljica-Žabčić, E.; Purgaric, B.; Kosar-Grašić, B.; Pavkovic, N. Precipitation of calcium phosphates from electrolyte solutions—IV. *J. Inorg. Nucl. Chem.* **1975**, *37*, 2047–2051. [[CrossRef](#)]
26. Füredi-Milhofer, H.; Purgaric, B.; Brečević, L.; Pavkovic, N. Precipitation of calcium phosphates from electrolyte solutions. *Calcif. Tissue Int.* **1971**, *8*, 142–153. [[CrossRef](#)]
27. Brečević, L.; Füredi-Milhofer, H. Precipitation of calcium phosphates from electrolyte solutions. *Calcif. Tissue Int.* **1972**, *10*, 82–90. [[CrossRef](#)]
28. Meić, I.B.; Kontrec, J.; Jurašin, D.D.; Džakula, B.N.; Štajner, L.; Lyons, D.M.; Sikirić, M.D.; Kralj, D. Comparative Study of Calcium Carbonates and Calcium Phosphates Precipitation in Model Systems Mimicking the Inorganic Environment for Biomineralization. *Cryst. Growth Des.* **2017**, *17*, 1103–1117. [[CrossRef](#)]
29. Nikolenko, M.V.; Esajenko, E. Surface Properties of Synthetic Calcium Hydroxyapatite. *Adsorpt. Sci. Technol.* **2005**, *23*, 543–553. [[CrossRef](#)]
30. Sutter, J.R.; McDowell, H.; Brown, W.E. Solubility study of calcium hydrogen phosphate. Ion-pair formation. *Inorg. Chem.* **1971**, *10*, 1638–1643. [[CrossRef](#)]
31. Tas, A.C. Monetite ( $CaHPO_4$ ) Synthesis in Ethanol at Room Temperature. *J. Am. Ceram. Soc.* **2009**, *92*, 2907–2912. [[CrossRef](#)]



32. Bakan, F. A Systematic Study of the Effect of pH on the Initialization of Ca-deficient Hydroxyapatite to  $\beta$ -TCP Nanoparticles. *Materials* **2019**, *12*, 354. [[CrossRef](#)] [[PubMed](#)]
33. Tao, J.; Jiang, W.; Zhai, H.; Pan, H.; Xu, X.; Tang, R. Structural Components and Anisotropic Dissolution Behaviors in One Hexagonal Single Crystal of  $\beta$ -Tricalcium Phosphate. *Cryst. Growth Des.* **2008**, *8*, 2227–2234. [[CrossRef](#)]
34. Tao, J.; Pan, H.; Zhai, H.; Wang, J.; Li, L.; Wu, J.; Jiang, W.; Xu, X.; Tang, R. Controls of Tricalcium Phosphate Single-Crystal Formation from Its Amorphous Precursor by Interfacial Energy. *Cryst. Growth Des.* **2009**, *9*, 3154–3160. [[CrossRef](#)]
35. Čadež, V.; Erceg, I.; Selmani, A.; Jurašin, D.D.; Šegota, S.; Lyons, D.M.; Kralj, D.; Sikirić, M.D. Amorphous Calcium Phosphate Formation and Aggregation Process Revealed by Light Scattering Techniques. *Crystals* **2018**, *8*, 254. [[CrossRef](#)]
36. Le Geros, R.Z. Variations in the Crystalline Components of Human Dental Calculus: I. Crystallographic and Spectroscopic Methods of Analysis. *J. Dent. Res.* **1974**, *53*, 45–50. [[CrossRef](#)]
37. Nakahira, A.; Aoki, S.; Sakamoto, K.; Yamaguchi, S. Synthesis and evaluation of various layered octacalcium phosphates by wet-chemical processing. *J. Mater. Sci. Mater. Electron.* **2001**, *12*, 793–800. [[CrossRef](#)]
38. Arellano-Jimenez, M.; Garcia-Garcia, R.; Reyes-Gasga, J. Synthesis and hydrolysis of octacalcium phosphate and its characterization by electron microscopy and X-ray diffraction. *J. Phys. Chem. Solids* **2009**, *70*, 390–395. [[CrossRef](#)]
39. Suzuki, O. Octacalcium phosphate: Osteoconductivity and crystal chemistry. *Acta Biomater.* **2010**, *6*, 3379–3387. [[CrossRef](#)]
40. Brown, P.W.; Martin, R.I. An Analysis of Hydroxyapatite Surface Layer Formation. *J. Phys. Chem. B* **1999**, *103*, 1671–1675. [[CrossRef](#)]
41. Mayer, I.; Jacobsohn, O.; Niazov, T.; Werckmann, J.; Iliescu, M.; Richard-Plouet, M.; Burghaus, O.; Reinen, D. Manganese in Precipitated Hydroxyapatites. *Eur. J. Inorg. Chem.* **2003**, *2003*, 1445–1451. [[CrossRef](#)]
42. TenHuisen, K. Formation of calcium-deficient hydroxyapatite from  $\alpha$ -tricalcium phosphate. *Biomaterials* **1998**, *19*, 2209–2217. [[CrossRef](#)]
43. Durucan, C.; Brown, P.W.  $\alpha$ -Tricalcium phosphate hydrolysis to hydroxyapatite at and near physiological temperature. *J. Mater. Sci. Mater. Med.* **2000**, *11*, 365–371. [[CrossRef](#)] [[PubMed](#)]
44. Durucan, C.; Brown, P.W. Kinetic Model for  $\alpha$ -Tricalcium Phosphate Hydrolysis. *J. Am. Ceram. Soc.* **2002**, *85*, 2013–2018. [[CrossRef](#)]
45. Vallet-Regí, M. Synthesis and characterisation of calcium deficient apatite. *Solid State Ion.* **1997**, *101*, 1279–1285. [[CrossRef](#)]
46. Siddharthan, A.; Seshadri, S.K.; Kumar, T.S.S. Microwave accelerated synthesis of nanosized calcium deficient hydroxyapatite. *J. Mater. Sci. Mater. Electron.* **2004**, *15*, 1279–1284. [[CrossRef](#)]
47. Hutchens, S.A.; Benson, R.; Evans, B.R.; O'Neill, H.M.; Rawn, C.J. Biomimetic synthesis of calcium-deficient hydroxyapatite in a natural hydrogel. *Biomaterials* **2006**, *27*, 4661–4670. [[CrossRef](#)]
48. Mochales, C.; Wilson, R.M.; Dowker, S.E.; Ginebra, M.P. Dry mechanosynthesis of nanocrystalline calcium deficient hydroxyapatite: Structural characterisation. *J. Alloys Compd.* **2011**, *509*, 7389–7394. [[CrossRef](#)]
49. Markovic, M.; Fowler, B.O.; Tung, M.S. Preparation and comprehensive characterization of a calcium hydroxyapatite reference material. *J. Res. Natl. Inst. Stand. Technol.* **2004**, *109*, 553–568. [[CrossRef](#)]
50. Narasraju, T.S.B.; Phebe, D.E. Some physico-chemical aspects of hydroxylapatite. *J. Mater. Sci.* **1996**, *31*, 1–21. [[CrossRef](#)]
51. Riman, R. Solution synthesis of hydroxyapatite designer particulates. *Solid State Ion.* **2002**, *151*, 393–402. [[CrossRef](#)]
52. Nancollas, G.; Wu, W.; Tang, R. The Control of Mineralization on Natural and Implant Surfaces. *MRS Proc.* **1999**, *599*, 99. [[CrossRef](#)]
53. Norton, J.; Malik, K.R.; Darr, J.A.; Rehman, I. Recent developments in processing and surface modification of hydroxyapatite. *Adv. Appl. Ceram.* **2006**, *105*, 113–139. [[CrossRef](#)]
54. Vázquez, N.S.G.; Luque, P.; Gomez-Gutierrez, C.M.; Olivás, O.D.J.N.; Sánchez, R.C.V.; Vilchis-Nestor, A.R.; Chinchillas, M.D.J.C. Hydroxyapatite Biosynthesis Obtained from Sea Urchin Spines (*Strongylocentrotus purpuratus*): Effect of Synthesis Temperature. *Processes* **2020**, *8*, 486. [[CrossRef](#)]
55. Rakovan, J. Growth and Surface Properties of Apatite. *Rev. Miner. Geochem.* **2002**, *48*, 51–86. [[CrossRef](#)]

56. Pan, H.-B.; Darvell, B. Solubility of hydroxyapatite by solid titration at pH 3–4. *Arch. Oral Biol.* **2007**, *52*, 618–624. [[CrossRef](#)]
57. Tsevis, A.; Spanos, N.; Koutsoukos, P.G.; Van Der Linde, A.J.; Lyklema, J. Preparation and characterization of anatase powders. *J. Chem. Soc. Faraday Trans.* **1998**, *94*, 295–300. [[CrossRef](#)]
58. Nikolenko, N.V.; Taran, I.B.; Plaksienko, I.L.; Vorob'ev, N.K.; Oleinik, T.A. Adsorption of organic compounds from aqueous solutions on silica gel and  $\alpha$ -aluminum oxide: A charge control model. *Colloid J. Russ. Acad. Sci. Kolloidn. Zhurnal* **1999**, *61*, 488–491.
59. Nikolenko, N.V.; Aksenenko, E.V.; Tarasevich, Y.I.; Dubenko, A.V.; Malakhova, E.V. Charge-controlled adsorption for wide-gap polar adsorbents. *Vopr. Khimii I Khimicheskoi Tekhnologii* **2018**, *5*, 37–45.
60. Nikolenko, N.V.; Shapovalova, I.M.; Kuprin, V.P. Model of charge controlled hydration for polar organic compounds. *Ukr. Chem. J.* **2002**, *68*, 113–116.



© 2020 by the authors. Licensee MDPI, Basel, Switzerland. This article is an open access article distributed under the terms and conditions of the Creative Commons Attribution (CC BY) license (<http://creativecommons.org/licenses/by/4.0/>).